Report of the ALMA Scientific Advisory Committee: September 2002 Meeting

October 15, 2002

ALMA Scientific Advisory Committee

ASAC Members

R. Bachiller (Spain), A. Benz (Switzerland), G. Blake (USA), R. Booth (Sweden), L. Bronfman (Chile), P. Cox (France, Chair), R. Crutcher (USA), N. Evans (USA), M. Gurwell (USA)*, D. Mardones (Chile), J. Richer (UK), P. Schilke (Germany), L. Mundy (USA), E. van Dishoeck (Netherlands), M. Walmsley (Italy), D. Wilner (USA), C. Wilson (Canada, Vice Chair), M. Yun (USA)

ASAC Observers

Y. Fukui (Japan), H. Matsuo (Japan)*, N. Nakai (Japan), S. Sakamoto (Japan), K. Tatematsu (Japan), M. Tsuboi (Japan)*, S. Yamamoto (Japan, Lead Observer)

Ex-officio Members

S. Guilloteau (ESO), R. Kawabe (Japan), T. Hasegawa (Japan), J. Mangum (NRAO), P. Shaver (ESO)*, A. Wootten (NRAO)

Other Participants

Members of the ALMA Project

B. Butler (NRAO), C. Cunningham (NRC), B. Glendenning (NRAO), R. Heald (NRAO), M. Holdaway (NRAO), R. Kurz (ESO), R. Lucas (IRAM), J. Kingsley (Tucson), R. Marson (NRAO), S. Myers (NRAO), S. Radford (NRAO), M. Rafal (NRAO), R. Simon (NRAO), D. Sramek (NRAO), M. Tarenghi (ESO), P. Vanden Bout (NRAO)

Others

C. Brogan (NRAO), C. Chandler (NRAO), D. Frail (NRAO), M. Goss (NRAO), M. Ishiguro (NAOJ), K. Johnson (NRAO), K.Y. Lo (NRAO), P. Napier (NRAO), M. Rupen (NRAO), E. Schinnerer (NRAO), D. Shepherd (NRAO), J. Ulvestad (NRAO), F. Walter (NRAO)

* Not present at Socorro meeting, but provided input to ASAC report.

APPENDICES

A. Report of the ASAC Subcommittee on Site and Stringency

A.1. Introduction

The ACC charged the ASAC to address the following issue:

The ASAC is asked to evaluate all available site (225 GHz opacity, 12 GHz phase stability, 350 micron and > 1 THz) data for Chajnantor, and to discuss any significant trends and issues which may impact the scientific mission, design or mission emphasis of the baseline instrument.

This issue was considered closely related to the considerations of stringency that have emerged from our thinking about operations and scheduling. Consequently, the ASAC asked that the definition of stringency be considered as part of this work.

The ASAC appointed a committee to address this issue, consisting of five ASAC members (Neal Evans, Chris Wilson, John Richer, Seiichi Sakamoto, and Diego Mardones), Simon Radford, Selby Cull (a summer student at NRAO-Tucson), and Robert Lucas. The ASAC members have supplied sample experiments that explore the parameter space of stringency. Radford and Cull have analyzed the site statistics. Lucas has considered the effect of these considerations on the ALMA simulator (delivering stringency estimates) and dynamic scheduler (incorporating stringency into the scheduler).

The committee decided to retain the definition of stringency in the Fall 2002 ASAC report:

$$S = t_a/t_p,$$

where t_a is the total available time and t_p is the total time during which the conditions for the observations are met. After discussing the available site statistics, we decided to estimate S based on the NRAO site statistics on $\tau(225)$, ϕ_{rms}, and wind speed accumulated since 1995. While there are other data from Pampa La Bola, the time base is shorter, so we deferred incorporation of those data.

The wind data are used to ask whether the primary pointing specifications are met; that is, we restrict ourselves to an either/or decision. If the wind is less than 6 m s^{-1} in the daytime or 9 m s^{-1} in the nighttime, we assume the pointing specification of 0.6 arcseconds to be met. This simple assumption is satisfactory for now, but it should be reassessed once the actual performance of the antennas is determined.

The yes/no wind criterion leaves two continuous variables. While there are diurnal, seasonal, and longer trends, we focus on the aggregate data over the period since 1995. Diurnal and seasonal trends are clearly present, as shown below; these may need to be considered in detailed planning. It is possible to compute S from the fraction of the time that both $\tau(225)$ and ϕ_{rms} are less than given values. We will show the joint distribution function for these two quantities in the last two figures. S will be the cumulative function computed from these distribution functions. We also supply relations to relate the effective seeing angle ($\theta(see)$) to the phase noise. We also discuss improvements due to the water vapor radiometers and/or fast switching.

Next we present the example observations. The site statistics and stringency results are presented in the following section, followed by a discussion of the effects of phase correction. Then there is a discussion of the consequences for software and conclusions.

A.2. Examples of Observations

1. This will be a modest stringency experiment. Detect absorption by molecular line against the continuum of a disk. The model is the detection of formaldehyde at 1.3 mm in IRAS4A by Di Francesco et al. 2001, ApJ 562, 770. Using IRAM, they detected H_2CO absorption at 1.3 mm of $T_b = 10$ K against a continuum of 3000 mJy. They used a velocity resolution of 0.16 km/s. This provides the best evidence for infall, but it is currently only possible for the few brightest sources. To generalize the result and to study the infall velocity field in detail, we would like to do similar experiments on sources with 10 times weaker disks with velocity resolution of 0.05 km/s. Thus we need rms noise of 0.1 K for 10 sigma detection. This could be done with modest spatial resolution, such as 1". Then we estimate the rms noise for 1 km/s resolution at 1.3 mm to be 0.29 K in 1 min. That indicates 168 min or 2.8 hours to achieve rms noise of 0.1 K with spectral resolution of 0.05 km/s and spatial resolution of 1". Since we are working at 1.3mm, the constraint on tau is very modest, say less than 0.1. Seeing constraint is also modest at say 0.5". Pointing just needs to meet spec. With the equations given below, the seeing constraint translates to a measured $\phi_{rms} = 3.2\,\mathrm{deg}$.

2. This will be about the highest stringency. We want to map a disk at the highest possible resolution. That means going to 0.35 mm in the largest array. Some probably out-of-date calculations indicate that we get a beam of 8.6 mas or 1.2 AU at 140 pc and can detect 71 earth masses of gas plus dust in 1 min. So we need the best tau and seeing, with great phase correction, and pointing in spec. Using the Matsushita conversion to 875GHz, we need $\tau(225) < 0.043$ to get $\tau(875GHz) < 1$. To get down to say 8 M_{earth}, we need these conditions for 1 hour. Let us say that we need $\theta(see) = 5$ mas. This translates to $\phi_{rms} = 0.12\,\mathrm{deg}$.

3. A deeply dust enshrouded super star cluster may only be detectable in the mm/submm continuum. To clearly identify such a cluster requires a spatial resolution of roughly 1 pc at a distance of 10-20 Mpc for typical cluster-containing galaxies. So we need angular resolution of 0.01-0.02$''$ and sufficient sensitivity to detect a dust signal that is equivalent to at least 10^6 and preferably 10^5 or 10^4 solar masses of gas. At 850 microns, this requires us to detect a source of 50-250 μJy at, say, the 5 σ level in continuum. Primary stringency requirement: atmospheric stability to get 0.01-0.02$''$ resolution at 850 microns. This translates to $\phi_{rms} = 0.26\,\mathrm{deg}$, and we take $\tau(225) = 0.1$ as our requirement.

4. A large population of faint submillimeter sources have been identified in the past 5 years using large single-dish telescopes. However, follow-up studies of this population have been limited because the poor angular resolution makes it difficult to identify optical and near-infrared counterparts. Obtaining accurate positions for these faint submillimeter sources should be easy with ALMA. For example, suppose we wanted accurate positions for 100 sources with 850 micron fluxes around 3 mJy. To get positions to roughly 0.1$''$ would require a resolution of 1$''$ and a signal-to-noise of about 10. To achieve this requires only 10 seconds per source with the full ALMA (20 minutes total plus overheads) or roughly 7 minutes per source with a 12-element "early" ALMA (11 hours total). These observations require moderate $\tau(225)$ ($< 0.1 - 0.15$) and moderately good seeing ($\phi_{rms} = 2.1\,\mathrm{deg}$). This experiment might be possible even if the seeing is not within the primary specification.

A.3. Site Characteristics

A.3.1. Background

On a high altitude (5050 m) plateau near Cerro Chajnantor in the Andes of northern Chile, the ALMA site is one of the best known locations for astronomy at millimeter and submillimeter wavelengths. Atmospheric conditions at Chajnantor have been studied extensively during the ALMA development phase and have been reviewed elsewhere (Radford & Holdaway 1998, Radford 2002). NRAO installed an instrument suite in 1995 April and ESO installed complementary instruments in 1998 June. On Pampa la Bola, about 8 km NE of the ALMA site, the Japanese installed monitoring instruments in 1996 June and the ASTE telescope in 2002 February. The NRAO and ESO instruments include a 225 GHz tipping radiometer, two 11.2 GHz interferometers, two 183 GHz line radiometers, a 350μm broadband tipping radiometer, and meteorology instruments. In addition, two groups have measured the atmospheric brightness at submillimeter wavelengths with Fourier Transform Spectrometers at Chajnantor (Matsushita et al. 1999, Paine et al. 2000).

At both 225 GHz and 350μm, the atmospheric transparency at Chajnantor is better more often than at Mauna Kea (Fig. 1). Only the South Pole enjoys comparable conditions (Radford & Chamberlin 2000, Radford 2002). At Chajnantor, the transparency shows significant seasonal and diurnal variations. Conditions are consistently good from April through December but deterioriate during January, February, and March (Fig. 2). In northern Chile, the summer months are known paradoxically as the "Bolivian winter" because a shift in the atmospheric circulation patterns draws moist air over the Andes from the Amazon basin. There is considerable year-to-year variation in the severity of this summer season. Even during the worst months on record, however, the median 225 GHz optical depth at Chajnantor, $\tau_{225} \approx 0.3$, is comparable to good conditions at many established observatories for millimeter wavelength astronomy. Diurnal transparency variations (Fig. 3) lag behind the solar cycle, with the best conditions occurring around sunrise. The diurnal variations are weaker during the winter than during the summer.

At Chajnantor, the atmospheric phase fluctuations on 300 m baselines are measured at 11.2 GHz by small interferometers observing beacons broadcast by communications satellites. For millimeter wavelengths, at least, these measured fluctuations can be scaled linearly with frequency to estimate the conditions at higher frequencies. For submillimeter wavelengths, however, dispersion at the edges of the windows becomes significant (Holdaway & Pardo 2001), so the measurements provide an underestimate of observing conditions. The phase stability is better in winter (Fig. 4), the diurnal phase stability variation (Fig. 5) is larger than the seasonal variation, the diurnal variation is more pronounced in phase stability than in transparency, and the diurnal phase stability variation more nearly matches the solar cycle than the diurnal transparency variation.

A.3.2. Phase Fluctuations and Seeing

Two methods have been suggested to relate the measured fluctuations to image quality (Table 1). Holdaway and Owen (1995) estimated the highest frequency where the phase fluctuations on 300 m baselines would allow good imaging (30° r.m.s.) or any image reconstruction at all (70° r.m.s.). Masson (1994) extrapolated the temporal structure function of the observed fluctuations to estimate the baseline, $b_{\max}$, where the phase fluctuations at 345 GHz are 1 radian r.m.s. and the corresponding angular resolution limit, or seeing, $\theta(see) = 0.7\lambda/b_{\max} = 0.14'' \ \lambda(mm)/b_{\max}(km)$. Essentially, one is simply limited in resolution by the largest usable baseline. To calculate the largest usable baseline, we first need to scale the measured ϕ_{rms} in degrees to the observed airmass (A), frequency (ν) and baseline (b) from ϕ_{rms} at the site testing parameters ($A = 1.7$, $\nu = 11.2$ GHz, and $b = 0.3$ km). For this report, we use the following: $\phi_{rms}(A,\nu,b) = \phi_{rms}(1.7, 11.2, 0.3)(A/1.7)^{0.5}(\nu/11.2)(b/0.3km)^s$ where the phase noise is assumed to increase as the square root of the air mass, linearly with frequency, and with baseline as the power s. We then set the phase fluctuations to the largest allowable phase fluctuations (in the example given here, 1 rad) and solve for b_{max}: $b_{max} = 0.3\text{km}[(11.2GHz/\nu)(1.7/A)^{0.5}(57.3/\phi_{rms}(A,\nu,b)]^{1/s}$. Finally, $\theta(see) = 0.47''\lambda(mm)[(\nu/11.2GHz)(A/1.7)^{0.5}(\phi_{rms}/57.3)]^{1/s}$, where ϕ_{rms} is the value from the site testing interferometer (note however that in some plots, it is already corrected to $A = 1$). The value of s changes with baseline, but we will approximate it here by $s = 0.6$. This is the median exponent on the structure functions of the measured data (Holdaway and Pardo 2001). In Table 1 below, we apply these equations to the case of observing at 345 GHz ($\lambda = 0.87$ mm) at the zenith ($A = 1$); note that the ϕ_{rms} values in the table are already referred to the zenith! The equation becomes $\theta(see) = 0.093''(\phi_{rms})^{1.67}$ One can easily substitute for other observing parameters or assumptions about the structure function.

Most of the time at Chajnantor, phase stable observations are possible only for long wavelengths or short baselines. To achieve the ALMA performance goals, compensation for atmospheric phase fluctuations will be necessary much of the time for millimeter wavelengths and modest baselines and most of the time for submillimeter wavelengths and long baselines.

Because of differences in instrument configuration and other factors, it is more complicated to compare phase fluctuation measurements at different sites than transparency measurements. Nonetheless, a quick estimate based on Masson's method (1994) indicates the median limiting angular resolution at Chajnantor is about twice as good as at Mauna Kea.

Table 1: Chajnantor phase stablility

measured $\phi_{\rm rms}$			$\nu_{\rm limit}$ [GHz]		345 GHz	
	[μm]		30°	70°	$b_{\rm max}$ [m]	$\theta_{\rm see}$
75 %	394	5.3°	63	148	52	2.40″
50 %	187	2.5°	134	313	181	0.69″
25 %	89	1.2°	281	655	625	0.20″
10 %	49	0.7°	510	1189	1691	0.07″

$\phi_{\rm rms}$: r. m. s. fluctuations on a 300 m baseline at 11.198 GHz at 36° elevation over 10 min intervals **referenced to the zenith**. $\nu_{\rm limit}$: frequency limit for observations with specified r. m. s. phase fluctuations on 300 m baselines (Holdaway & Owen 1995). $b_{\rm max}$ [m] and $\theta_{\rm see}$: maximum usable baseline and effective seeing at 345 GHz (Masson 1994) calculated for the median structure function exponent, 0.6 (Holdaway and Pardo 2001).

A.3.3. Correlations

Several atmospheric parameters show significant correlation, but others are only weakly correlated at best. To illustrate these correlations in the presence of substantial scatter, the data were selected on the value of one parameter and then distributions of a second parameter were compiled. The comparisons show westerly winds are stronger than easterly winds (Fig. 6), the transparency is better during colder periods (Fig. 7) and during westerly winds (Fig. 8), and the phase stability is better during weaker winds (Fig. 9). and colder periods (Fig. 10). Despite a tremendous scatter, there is a significant correlation between the transparency and the phase stability. When the transparency is better than the median, the phase stability is about twice as good as otherwise (Fig. 11).

The atmospheric data are recorded every 10 min. To evaluate conditions over longer intervals, cumulative distributions were compiled for the median or the maximum during the interval. As expected, there is essentially no change in the distributions of the medians (Fig. 12). For the maxima, on the other hand, the distributions show a monotonic degradation with interval length (Fig. 13). This is more pronounced for the phase fluctuations than for the transparency (Fig. 14).

In Figure 15, we have plotted the two-dimensional probability density $P(\phi, \tau)$. The contours encircle 5, 10, 15, ... per cent of the total probability. Although typical conditions are of course excellent, there is a significant amount of time with less good conditions. Note especially the relatively long tail on the phase stability distribution. The correlation of τ and ϕ has substantial scatter. We have also shown the joint probability densities (Fig. 16) of the opacity and phase stability when the wind speed is such that the primary pointing specifications will be met (speed is > 6 m/s at day, or > 9 m/s at night time). Note that these wind conditions are met only 56% of the time, so the outermost contour is the 50% contour. Note the substantial growth in the contours, especially outside the 25% contour, when the wind condition is applied. Taken at face value, these statistics would suggest that up to 44% of the observing time could be lost to high winds. This suggestion is overly pessimistic. While the tighter wind limit in daytime was meant to allow for some pointing degradation because of thermal effects, there is a compensating effect: higher wind makes solar heating less localized. Thus, the wind limit may actually not be less in the daytime. If we arbitrarily adopt 9 m/s for daytime as well, only 30% of the time would be potentially lost, and much of that is in afternoons, when other conditions also degrade. In addition, the pointing is unlikely to degrade catastrophically as the primary wind limits are exceeded. It will be very useful to characterize the antenna pointing in winds over those limits.

A.4. Software implications

Requirements have been discussed by the SSR, and are available at

`http://iraux2.iram.fr/%7Elucas/almassr/report-2/report-2-v4r2.pdf` [1]

The sections relevant here are Dynamic Scheduling (3.4) and Simulation (3.8).

A.4.1. Dynamic Scheduling

Programmes will be split into scheduling blocks; the scheduling block priorities will be reevaluated at the end of execution of each block (long programmes will be obtained by repeated execution of the same block). The priorities will include many factors, some trivial (e.g., source visibility), other highly fluctuating like phase rms and system temperature (atmosphere included). Both science rating and stringency will be primary factors.

The SSR required that the dynamic scheduler should be its own simulator, as it can be executed with

[1] this link points to a new version of ALMA Software memo 11 that should still be regarded as a draft, until it is formally reviewed at the end of 2002 September; however this text takes into account the reviewers' comments.

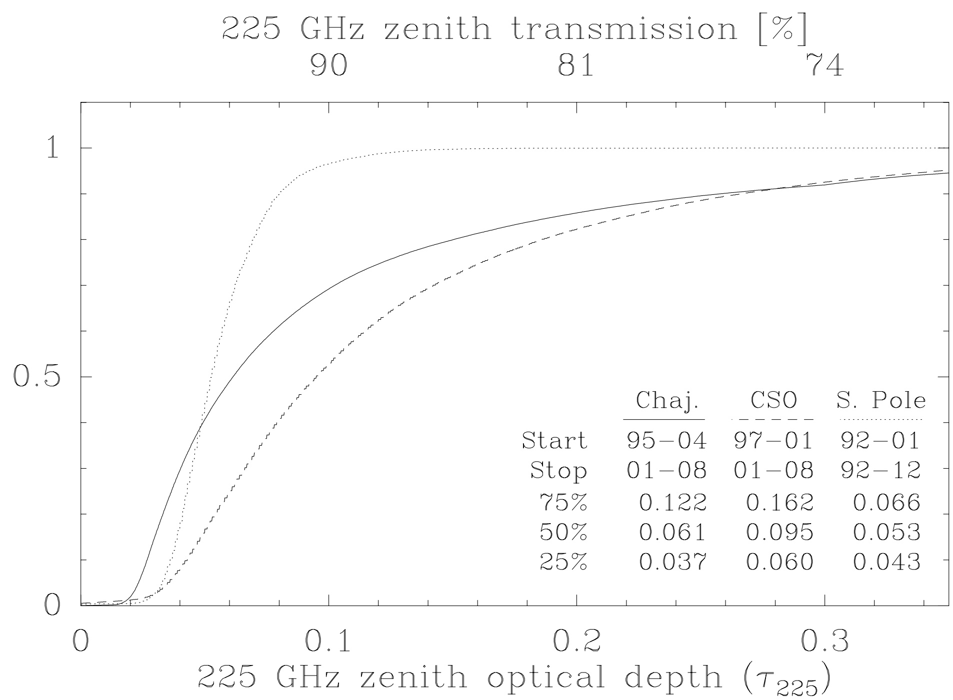

Fig. 1.— Cumulative distributions of the 225 GHz zenith optical depths (τ_{225}) measured at Chajnantor, at Mauna Kea (CSO), and at the South Pole. Adapted from Radford & Chamberlin (2000). The distributions of the broadband 350μm measurements are similar

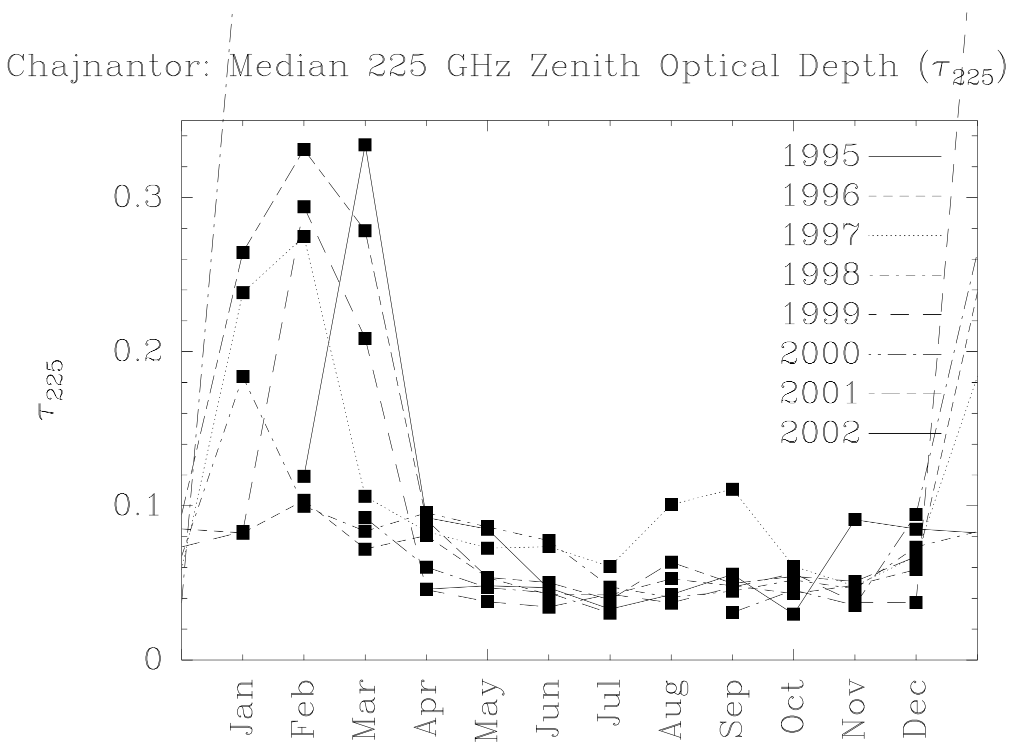

Fig. 2.— Seasonal variation of median measured 225 GHz zenith optical depths at Chajnantor. The variation of the broadband 350μm measurements is similar

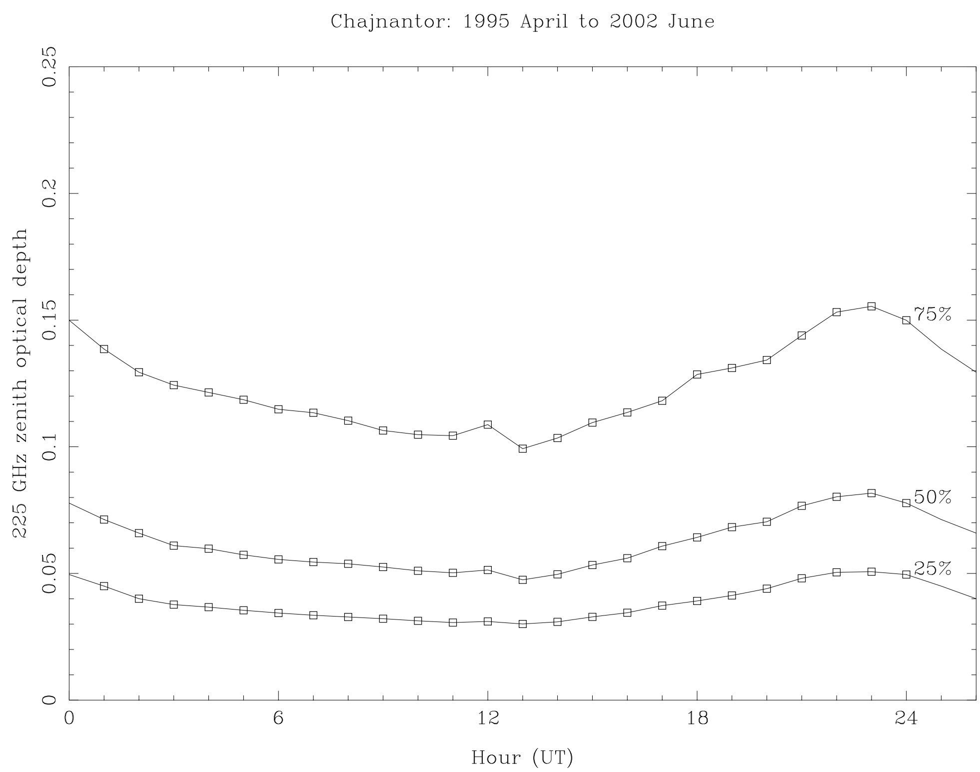

Fig. 3.— Diurnal variation of quartiles of measured 225 GHz zenith optical depths at Chajnantor. Local solar time is UT $- 4^{\rm h}\,31^{\rm m}$. The variation of the broadband 350μm measurements is similar.

atmospheric data (as we already have) and a set of scheduling blocks as input, to tune up the formula and coefficients for optimum use of ALMA during a scheduling season:

"The actual formula and coefficients must be tuned for optimum overall efficiency, and agreement with observatory policy, according to the distribution of programme requirements and the weather statistics on the ALMA site. The ordering of programmes according to scheduling probabilities should match that of science ratings, in each range of observing conditions."

The conclusions of the present report call for treating the system temperatures (or opacities) and the phase rms as truly independent parameters, which had been foreseen. They should both appear as strict upper limits (e.g., a Scheduling Block requiring less than 1 mm precipitable H_2O and 50μm pathlength rms is not scheduled if either requirement is not met) and through the stringency factor (to make sure this SB is given priority over less demanding ones whenever these conditions are met).

A.4.2. Simulation

Memo 11 formulates requirements on ALMA simulator. The simulator should in principle allow to investigate the use of both fast switching and radiometric phase correction methods, by generating fake data using state-of-the-art atmosphere models, and processing them through the off-line data reduction package.

A.5. Summary

The data presented above lead us to the following conclusions.

- There are no indications in the site weather data that the ALMA scientific mission or design needs to be changed.
- There is some correlation between good transmission and good phase noise. However there are significant periods when transmission is good, but phase noise is not very good.
- Examples of ALMA science indicate that some of the most exciting science cannot be done without the successful functioning of the phase correction scheme. Making this scheme work will also make the periods of good transmission but poor phase noise usable.
- Determining how the pointing actually degrades as wind conditions worsen will be important in assessing the fraction of time that can be used for different projects. In particular, the effects during daytime need further study.
- The ASAC encourages the ongoing study to simulate dynamic scheduling and recommends implementation of a full stringency calculator.

If we apply the calculations to the examples given in §A.2, we find that experiment number 1 can be done about 30% of the time; if the pointing degrades gracefully, this percentage could be increased. The fourth example could be done about 25% of the time. Neither of the other examples could be done without phase correction in any significant fraction of the time. Assuming that phase correction works to the levels needed, experiment number 2 could be done about 17% of the time and experiment number 3 could be done

39% of the time (these estimates include only the constraint on τ and assume that the pointing will be acceptable 56% of the time). These examples reinforce the conclusions drawn above.

We suggest that some of the issues raised in this study be pursued as future work. With the existing data, it would be useful to search for rapid time variations in the wind speed, opacity, and phase noise. In particular, rapid variations in phase noise may be ionospheric in origin; these would be less important at high frequencies. If they contribute significantly to the distribution of high $\phi(rms)$, those statistics could be too pessimistic. We recommend further study of the likely effect of wind on the antennas based on the detailed specifications. However, the most important thing will be to characterize the pointing degradation as winds exceed the nominal values for the primary pointing specfications. Finally, we encourage implementation of a stringency calculator based on input requirements and using the available site data. This should be coupled with the ongoing study of how dynamic scheduling will work.

References

Holdaway, M. A.& Owen, F. N., 1995, Millimeter Array Memo 136 (NRAO) *Correcting for Decorrelation Due to Atmospheric Phase Errors*

Holdaway, M. A.& Pardo, J. R., 2001, Atacama Large Millimeter Array Memo 404 (NRAO) *Atmospheric Dispersion and Fast Switching Phase Calibration*

Masson, C. R., 1994, in Astronomy with Millimeter and Submillimeter Wave Interferometry, IAU Colloquium 140, ASP Conference Series, Vol. 59, M. Ishiguro & J. Welch, Eds., p.87 *Atmospheric Effects and Calibrations*

Matsushita, S., Matsuo, H., Pardo, J. R., & Radford, S. J. E., 1999, PASJ 51, 603 *FTS Measurements of Submillimeter-Wave Atmospheric Opacity at Pampa la Bola II: Supra-Terahertz Windows and Model Fitting*

Paine, S., Blundell, R., Papa, D. C., Barrett, J. W., & Radford, S. J. E., 2000, PASP 112, 108 *A Fourier Transform Spectrometer for Measurement of Atmospheric Transmission at Submillimeter Wavelengths*

Radford, S. J. E., & Holdaway, M. A., 1998, in Advanced Technology MMW, Radio, and Terahertz Telescopes, ed. Phillips, T. G., Proc. SPIE 3357, 486 *Atmospheric Conditions at a Site for Submillimeter Wavelength Astronomy*

Radford, S. J. E., & Chamberlin, R. A., 2000, Atacama Large Millimeter Array Memo 334.1 (NRAO) *Atmopsheric Transparency at 225 GHz over Chajnantor, Mauna Kea, and the South Pole*

Radford, S., 2002, in Astronomical Site Evaluation in the Visible and Radio Range, ASP Conf. Ser. 266, ed. Vernin, J., Benkhaldoun, Z., & Muñoz-Tuñón, C. (San Francisco: ASP) p. 148 *Site Characterization for mm/submm Astronomy*

A. Report of the ASAC Subcommitte on Early Science with ALMA

A.1. Introduction

In June 2002, the ASAC was requested by the ACC to define the early science which could be started before the full completion of the ALMA baseline project. The charge is as follows:

The ASAC is requested to make an assessment of ALMA early science. What kinds of scientific data (including the balance between spectroscopic and continuum data) are likely to be most desired as ALMA begins operations? Based on this probable interest, what are the commissioning and operational implications for the array's baseline capabilities, frequency coverage and operating modes?

A working group was constituted with the following members: Pierre Cox, Stephane Guilloteau, Diego Mardones, Hiroshi Matsuo, Ken Tatematsu, Ewine van Dishoeck, Malcolm Walmsley, David Wilner, Christine Wilson, and Al Wootten. This is a progress report summarising the discussions and outlining some of the issues related to the Early Science with ALMA.

A.2. Definition, Requirements and Goals of Early Science

The main purpose of this document is to explore realistic goals for the early phases of ALMA scientific operations, before ALMA is sufficiently complete, where the term "sufficiently complete" should be defined, since no input definition has been given yet (see § A.6).

Early Science is *not* Commissioning (§ A.3). Early Science will involve the community, therefore implying that it will go through a phase of Call for Proposals, although perhaps in some restricted form, and that the programmes will be selected according to criteria to be defined.

The goals of Early Science are manifold and we recommend that they include:

- Early Science must demonstrate the *unique capabilities* and the scientific potential of ALMA by providing unique scientific results.
- Early Science should foster a *rapid scientific return* from ALMA, for a wide range of topics, from solar system physics (including the sun) to the high redshift universe.
- Early Science must show these capabilities to *all astronomers*, not only experts in millimeter/submillimeter astronomy, in order to involve scientists from a large community in a *prompt and efficient use of ALMA* and to familiarize the community with these new techniques.
- Early Science must produce *compelling images*, which is not only the best way to convince the community, in particular the optical astronomers, but will also catch the public's interest.
- Early Science must be used to provide *feedback* to ALMA on *operations* from the User Community.

A.3. Science Verification during Commissioning

The goals of Science Verification in the Commissioning are different from those of Early Science and are as follows:

- Science Verification must demonstrate the *basic* ALMA capabilities.
- Science Verification must test systematically the expected *operating modes* of ALMA.
- Science Verification must have a *verifiable output*, which should be made available to the community as the basis for advertising Early Science capabilities (in the Call for Proposals.)
- Results from the Science Verification could serve public relations purposes early on, as well as inviting Early Science proposals. Scientific topics could include first high quality images of Centaurus A, 30 Doradus, η Carina, or spectral line results, e.g., searches for pre-biotic molecules.

Science Verification during Commissioning is therefore closely linked with the ALMA operations and will only involve experts, i.e. people who are close to the instrument and the operations. However, Commissioning can be a phased activity overlapping with Early Science. When more ALMA capabilities become available, they first go through a phase of Commissioning, before being offered for Early Science.

A.4. Unique Capabilities of ALMA in Early Science

Prior to the start of operations of the full ALMA array, i.e. 64 antennas (at the end of 2011), ALMA will provide the community with capabilities exceeding those of current or planned millimeter/submillimeter arrays. Early Science will utilize the ALMA capabilities which have been demonstrated during Science Commissioning. Those capabilities include:

- **Sensitivity**

  From the first year of operation onwards the sensitivity of ALMA will exceed that of all existing or planned array in all 4 Priority Bands During the first year, the continuum sensitivity will be a factor 2-3 better due to the wide bandwidths, with only a slight improvement in spectral line sensitivity During the following years, as the number of antennas increases, the gain in both continuum and line sensitivities improves by a factor ≈ 2 at each step, approaching 50% of the ultimate sensitivity after the third year of operation (32 antennas). We note that besides offering the best continuum sensitivity, wide bandwidth will also be a major advantage for any spectral line survey.

- **Long Baselines**

  By 2007, ALMA will be equipped up to 4 km baselines, i.e. much longer than any array so far, and on a superior site. This will enable astronomers to achieve unprecedented spatial resolution at millimeter and submillimeter wavelengths. Using long baselines requires that phase correction techniques are operational and bringing those into operation should be planned for early on in the project.

- **Frequency Coverage**

  The frequency coverage offered by ALMA and the site characteristics of Chajnantor will allow astronomers to observe not only at millimeter wavelengths (1 and 3 mm) but also at high frequencies, i.e. using Bands 7 & 9 at 345 and 675 GHz, and explore the submillimeter domain at unprecedented spatial resolution and sensitivity (especially in the continuum). It should be noted that, even with 6 antennas, ALMA will have 3 times better continuum and line sensitivity at 345 and 675 GHz than the eSMA

- **Polarization**

  Although polarization measurements will build on the discoveries made by pioneering efforts on other arrays, polarization will certainly not be fully exploited when ALMA can start operations around 2007. Polarization is a crucial aspect of the ALMA capabilities, and its scientific verification should be planned early on.

- **Southern Sky Sources**

  The access to the southern Sky opens up the possibility to observe unique sources which are only (or best) visible in the southern hemisphere, such as the Galactic Center, the Magellanic Clouds, Centaurus A, some of the major star formation regions in the Southern sky, in particular the Carina Nebula (including the massive star η Car), the debris disk β Pictoris, and transient objects (comets).

- **Image Quality**

  As soon as the number of antennas exceed 15, the imaging quality will be better and the imaging speed will surpass by a large amount that of other instruments. However, the imaging quality may depend on the nature of the field being imaged.

- **Calibration Accuracy**

  The calibration goals of ALMA of 1% at millimeter wavelengths and 3% at submillimeter wavelengths are an order of magnitude better than at current millimeter observatories, allowing different types of science to be performed.

A.5. What should be avoided in Early Science

In Early Science at least two things should be avoided. First, there is no need in trying to obtain a result in, e.g., 3 months during the first year, while it could be obtained in a only a day once ALMA is completed. It is important to remember that with 6 antennas, ALMA will be 100 times slower than when fully completed. This implies that any experiment in the Early Science phase should not exceed 1 week of observing time. In particular, very extensive surveys should not be conducted. Second, imposing requirements which cannot be met should be avoided. In any case, during Early Science, priority should be given to science which makes the best use of ALMA's unique capabilities.

A.6. Steps and Duration of Early Science

Early Science starts as soon as 6 to 8 (or perhaps even more) antennas are available for science operations in Q3 2007. The reasons for starting with at least 6 antennas are: (i) ALMA with less than 6 antennas is not competitive scientifically in sensitivity and UV coverage compared with other facilities available in 2007; (ii) commissioning is a delicate problem and a learning curve is required; (iii) science commissioning requires 6 antennas to be operational to ensure most modes have been tested; and (iv) commissioning of additional antennas and/or receiver bands requires sub-array capabilities.

We recommend that commissioning of new telescopes and/or receivers is done in a separate sub-array and is not shared with Early Science. Thus, a minimum of 8 commissioned antennas (6 in main array for Early Science, 2 + new to be commissioned antenna in sub-array) will be necessary. In addition, it is desirable that 1 antenna equipped for total power observations should be available from the start. Once new antennas and/or receiver bands have been commissioned, they should be added to the science array as soon as possible, and in the case of the antennas in groups of 4, 6 or 8 antennas (rather than one by one). Early Science phases can be applied separately to different frequency bands.

We recommend that Early Science observing does not start with less than 2 receiver bands. For commissioning, the availability of Band 3 receivers is essential. As noted above, the largest gains in sensitivity and spatial resolution are obtained at the highest frequencies, but Band 9 will be technically challenging to commission in the first year. Experience at other observatories has shown that Band 7 should not be more difficult to commission than Band 6. Band 9 should nevertheless be tested and commissioned early-on, at least on a sub-array to characterize the antennas and site at the highest frequencies. The final choice of initial bands to be implemented must involve a trade-off between scientific, technical and programmatic arguments.

A natural end-point of Early Science is when 32 antennas have been commissioned, expected around late 2009. The reasons are: i) with 32 antennas the sensitivity is half of the final one; ii) the imaging quality is close to final.

A.7. Recommendations

Based on the discussions summarized in the previous sections, the ASAC makes the following recommendations concerning ALMA Early Science:

- Early Science should start with not less than 6 antennas, and preferably 8 to 10 antennas.
- Early Science should allow continuum and line observations from the start.
- Early Science should start with not less than two receiver bands, including Band 3.
- Phase correction is essential for Early Science observations.
- Early Science should include polarisation as soon as possible.
- The array for Early Science should be separated from the telescope's array for commissioning through sub-array capabilities.
- Additional antennas and/or receivers bands should be brought into the science array as soon as they have been commissioned. In the case of the antennas, it will likely be more efficient in terms of operations to bring them into the science array in small groups of 4, 6, or 8 antennas.
- The ASAC recommends having 1 antenna instrumented with total power mode capability for Early Science, if possible.

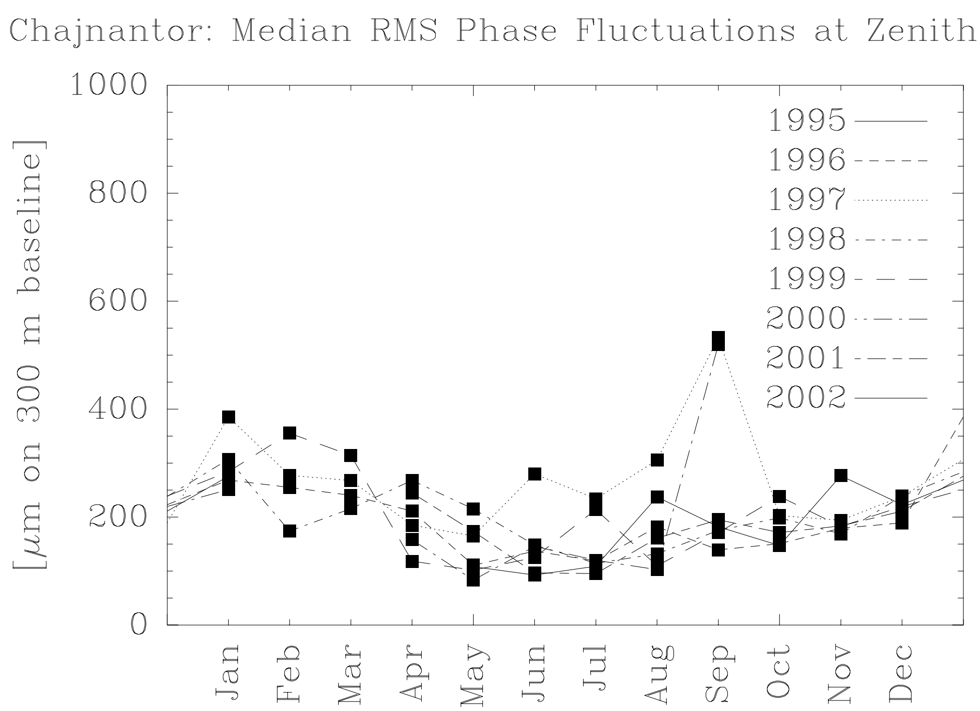

Fig. 4.— Seasonal variation of median measured phase fluctuations at Chajnantor referred to the zenith.

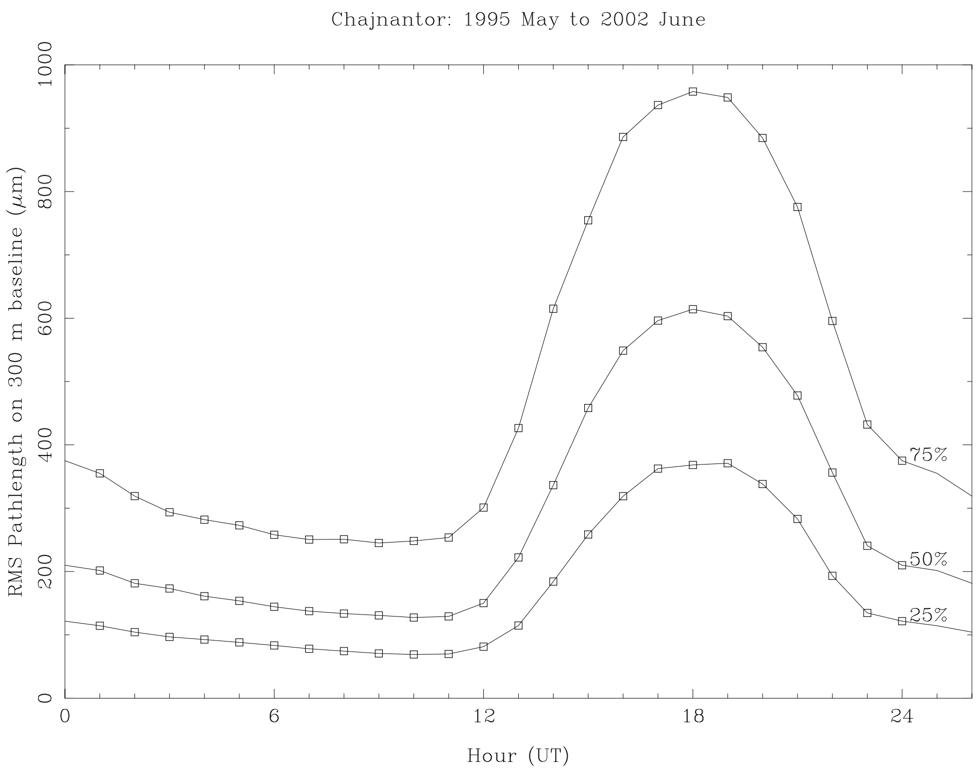

Fig. 5.— Diurnal variation of quartiles of measured phase fluctuations at Chajnantor referred to the zenith.

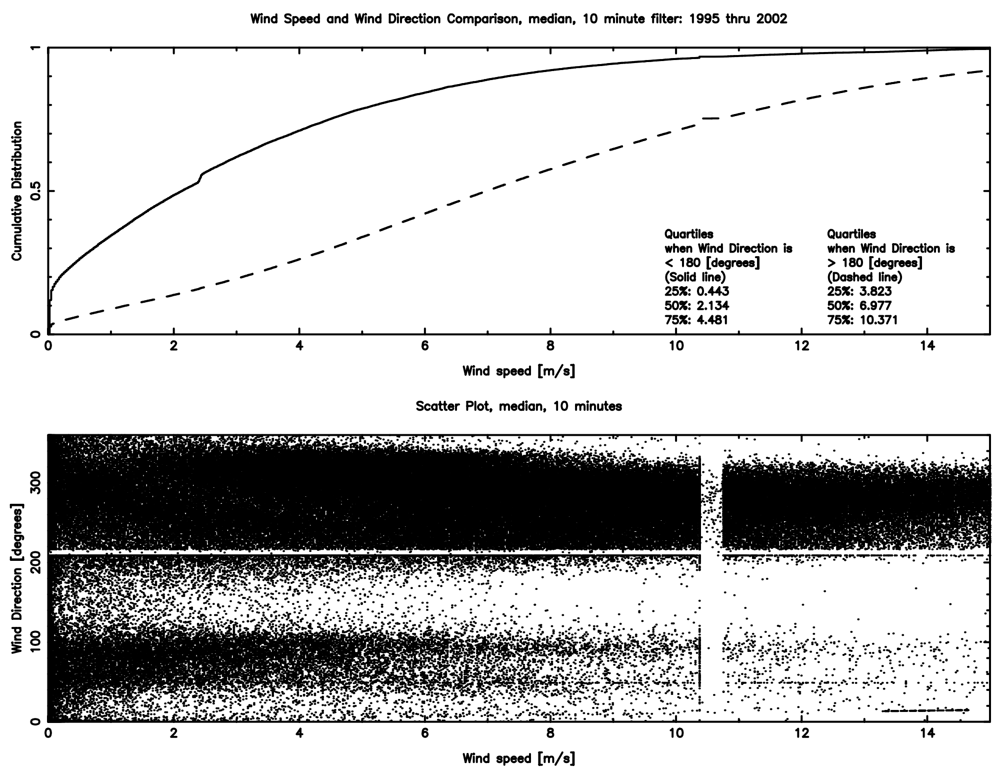

Fig. 6.— Cumulative distributions of westerly and easterly wind speeds measured at Chajnantor.

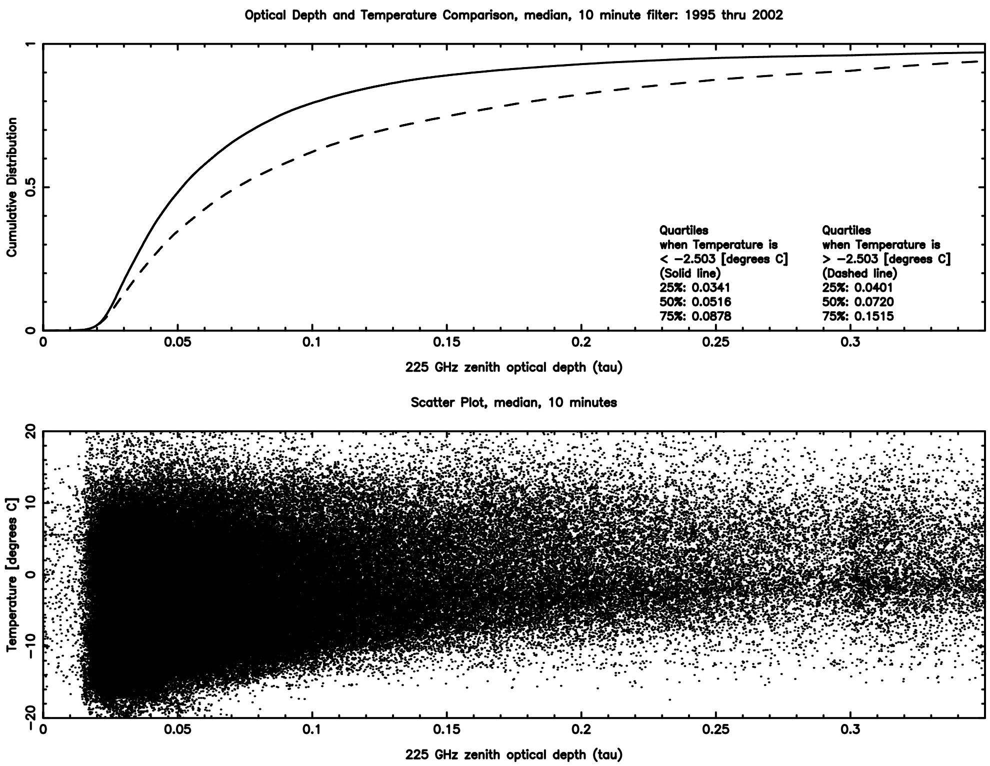

Fig. 7.— Cumulative distributions of the 225 GHz zenith optical depths (τ_{225}) measured at Chajnantor when the temperature was above or below the median.

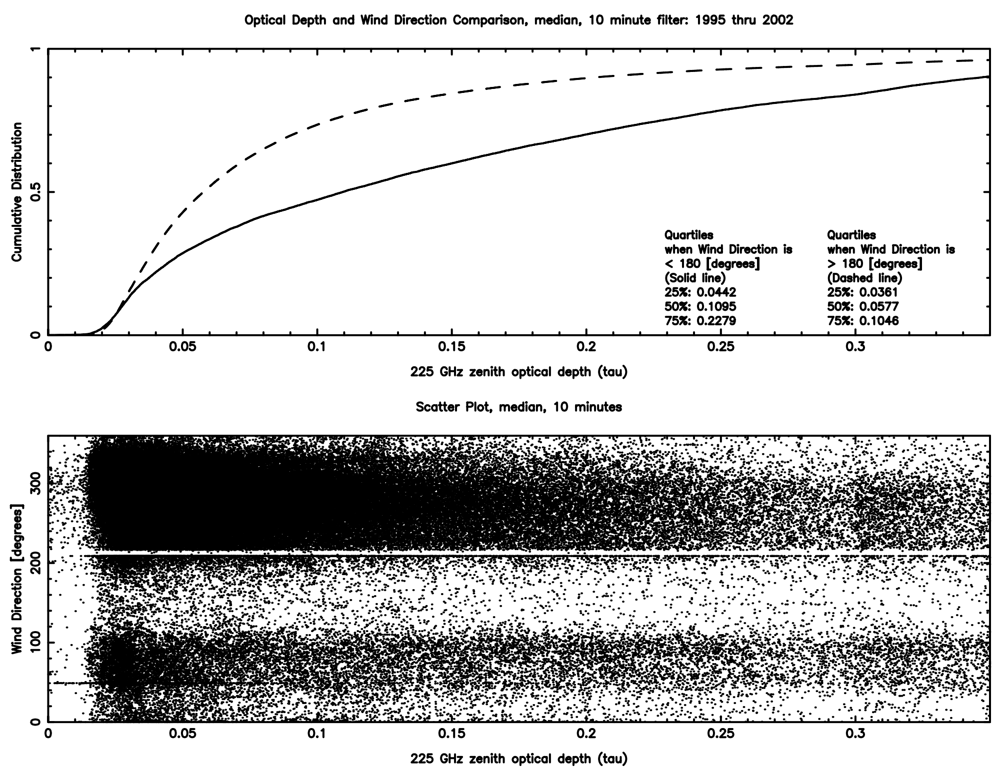

Fig. 8.— Cumulative distributions of the 225 GHz zenith optical depths (τ_{225}) measured at Chajnantor during westerly and easterly winds.

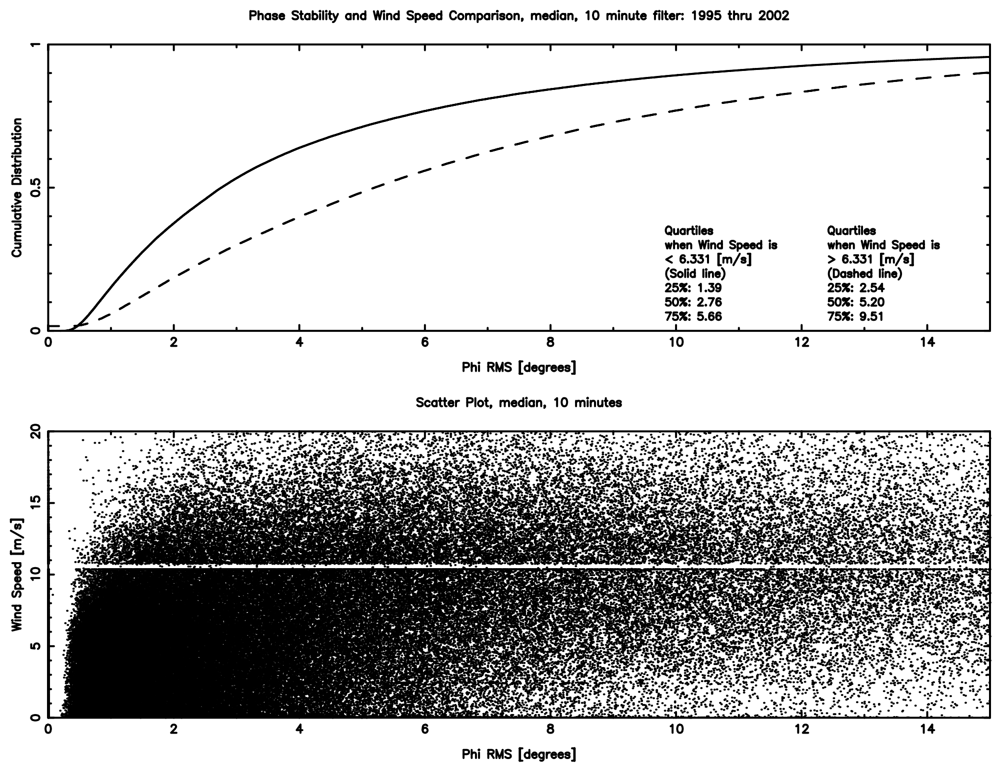

Fig. 9.— Cumulative distributions of the maximum 11.2 GHz phase fluctuations measured at Chajnantor when the wind speed was above or below the median.

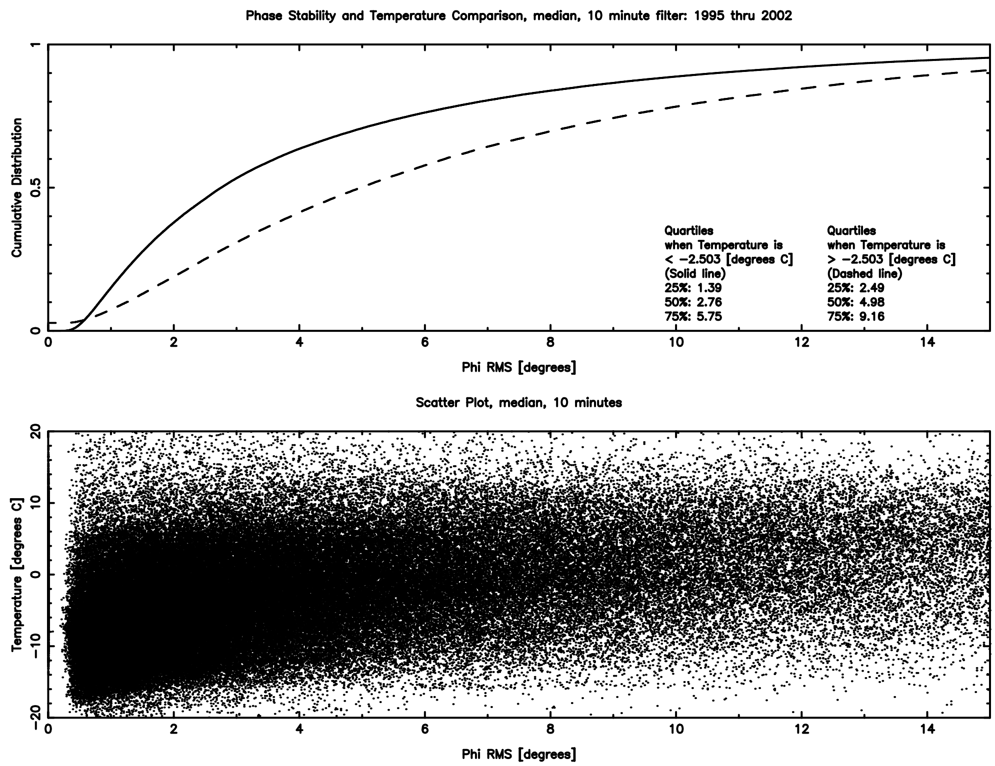

Fig. 10.— Cumulative distributions of the maximum 11.2 GHz phase fluctuations measured at Chajnantor when the temperature was above or below the median.

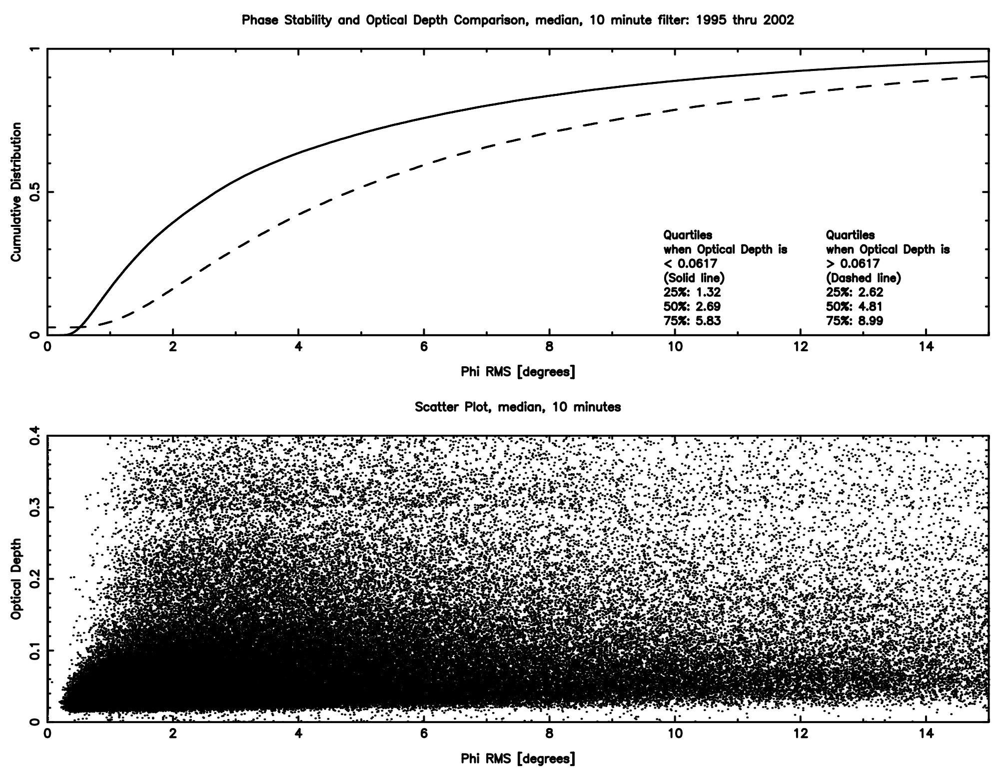

Fig. 11.— Cumulative distributions of the maximum 11.2 GHz phase fluctuations measured at Chajnantor when the 225 GHz zenith optical depth (τ_{225}) was above or below the median.

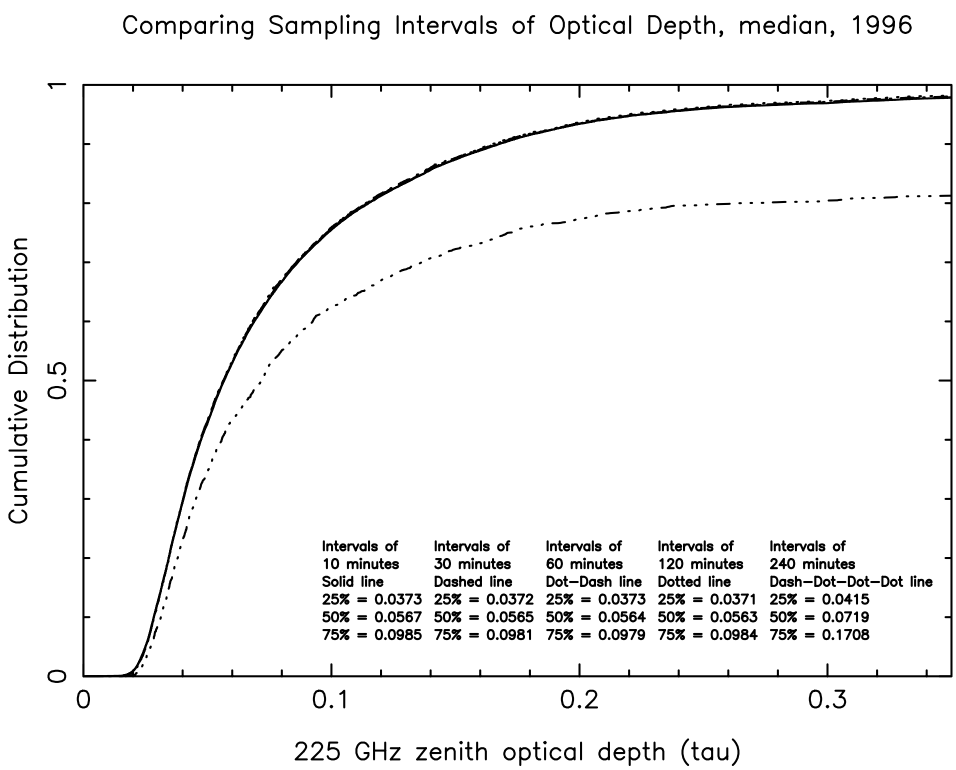

Fig. 12.— Cumulative distributions of the median 225 GHz zenith optical depths (τ_{225}) measured at Chajnantor in 1996 for different sampling intervals. The 240 min interval suffers from a processing defect.

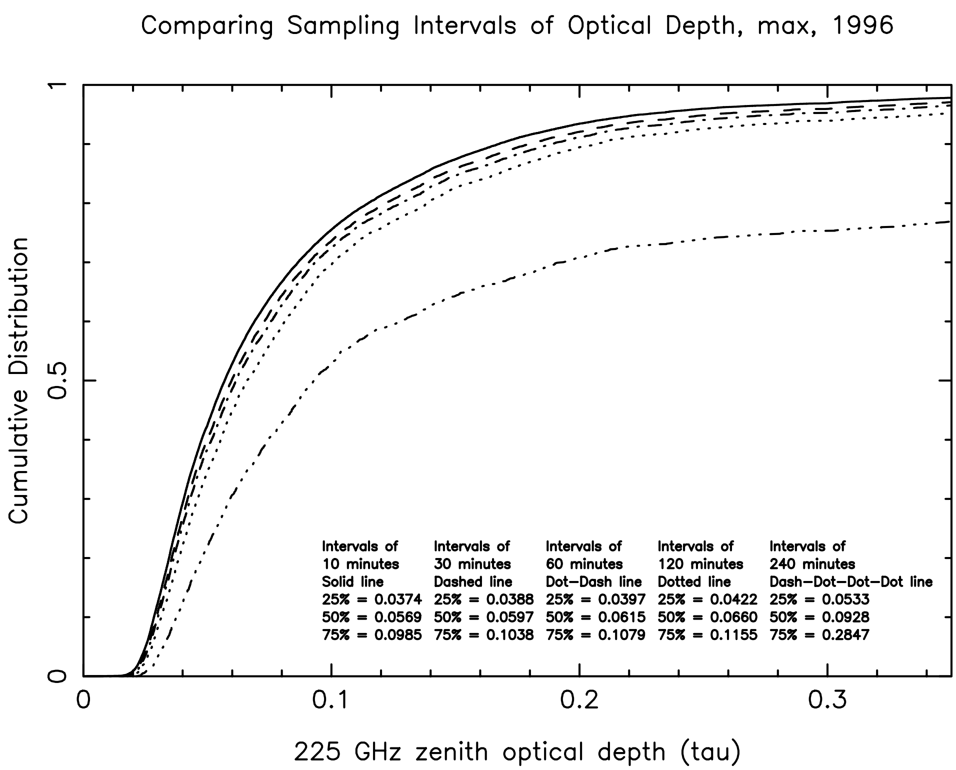

Fig. 13.— Cumulative distributions of the maximum 225 GHz zenith optical depths (τ_{225}) measured at Chajnantor in 1996 for different sampling intervals. The 240 min interval suffers from a processing defect.

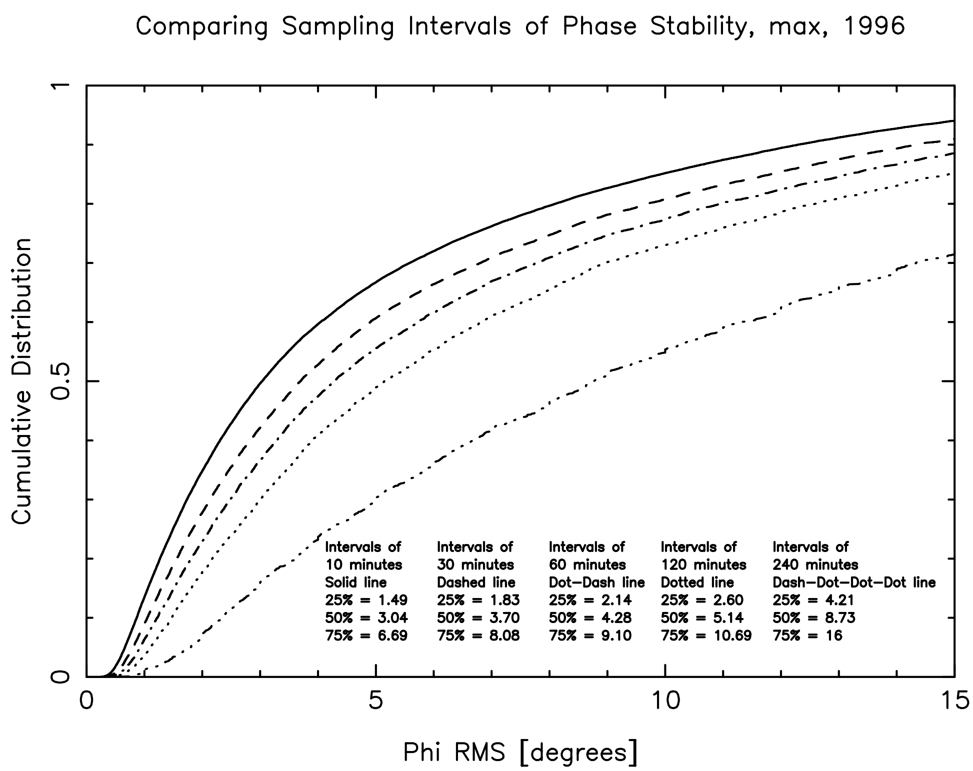

Fig. 14.— Cumulative distributions of the maximum 11.2 GHz phase fluctuations measured at Chajnantor in 1996 for different sampling intervals. The 240 min interval suffers from a processing defect.

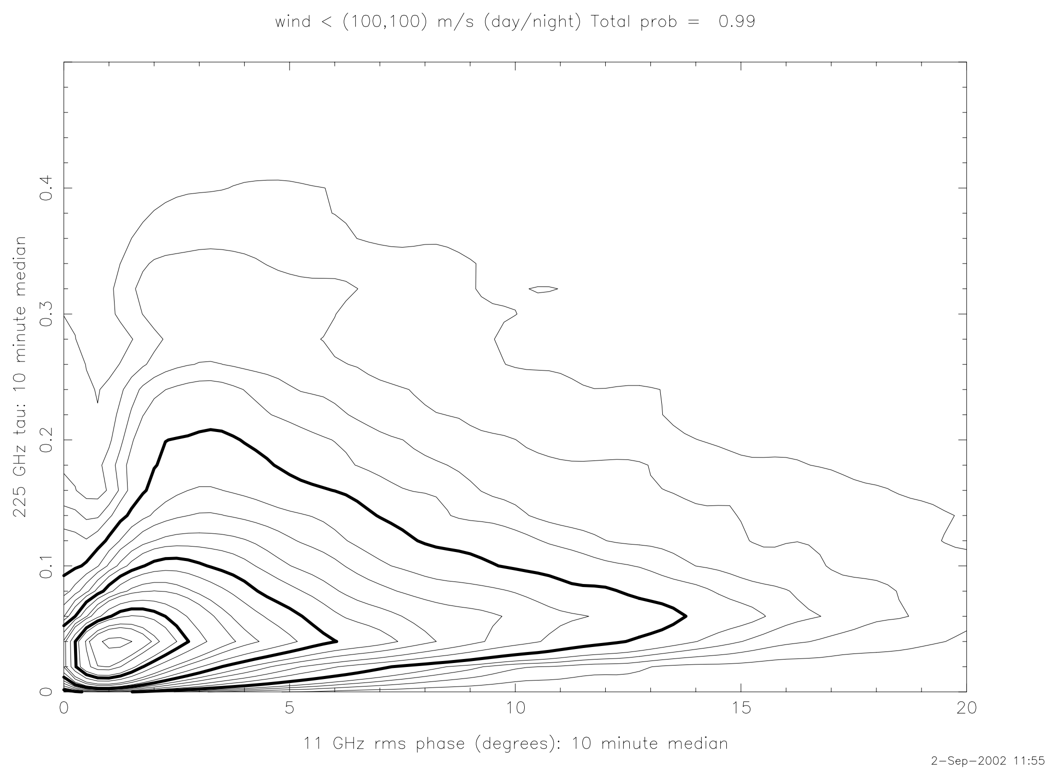

Fig. 15.— Joint probability distribution of $\tau(225)$ and $\phi(rms)$ with a very loose wind (pointing) requirement: that the wind speed be less than 100 m/s either day or night. The contours encircle 5, 10, 15, … per cent of the total probability (99% in this case).

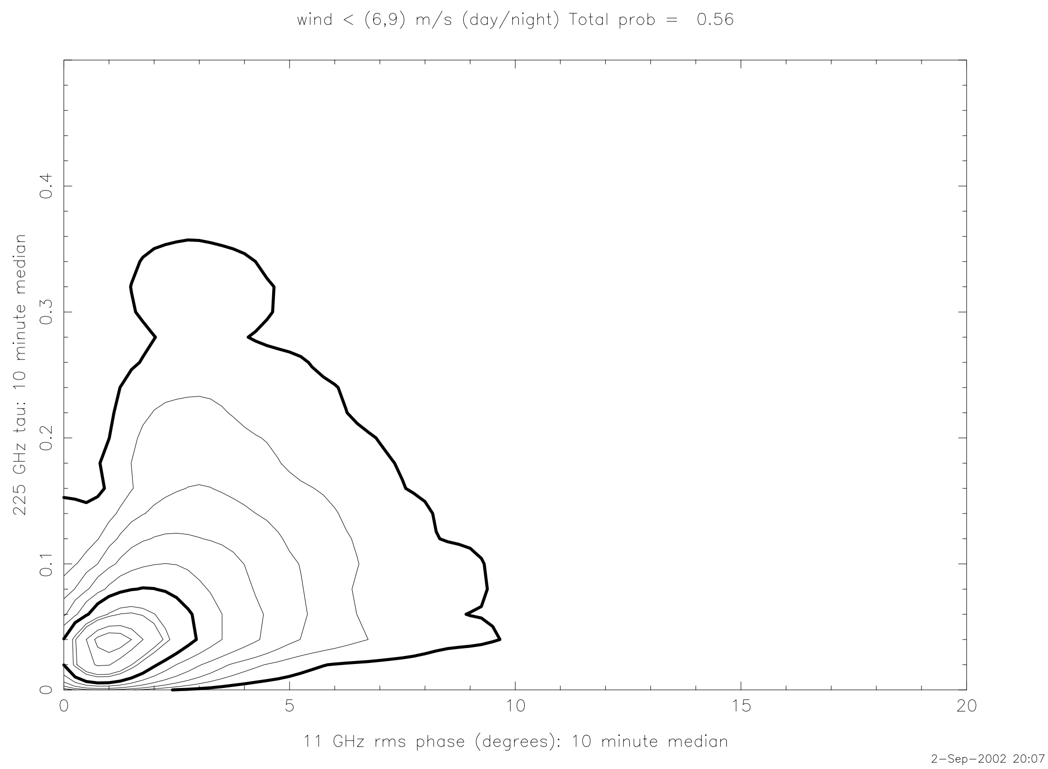

Fig. 16.— Joint probability distribution of $\tau(225)$ and $\phi(rms)$ with a the wind requirement that allows the pointing specification to be met: that the wind speed be less than 6 m/s in the daytime and less than 9 m/s at night. The contours encircle 5, 10, 15, … per cent of the total probability (55% in this case).